

<https://doi.org/10.1038/s42003-025-08526-6>

Agxt2l-mediated glycerophospholipid metabolism in trophocytes explains *Apis mellifera* queen's higher oviposition over *A. cerana*

Check for updates

Luxia Pan^{1,2,3,4}, Zilong Wang^{1,3,4}, Shiqing Zhong^{1,3,4}, Tianyu Xu^{1,3}, Weixuan Chen^{1,3}, Fuping Cheng^{1,3} & Zhijiang Zeng^{1,3} ✉

Apis mellifera and *Apis cerana* are two important honey bee species widely kept and studied. But their queens differ greatly in egg-laying capacity. To determine the mechanisms of this difference, we compare gene expression, chromatin accessibility and spatial localization of differential genes in the ovaries of the two species in virgin queens and laying queens using ATAC-seq, RNA-Seq, homologous gene alignment and spatial transcriptome. The results reconfirm that the egg-laying capability of *A. mellifera* queens is significantly higher than that of *A. cerana* queens. The chromatin accessibility and nutrient cells ratio of *A. mellifera* queens are higher than those of *A. cerana* queens. Further investigations reveal that *agxt2l* (*LOC408817*) is significantly over-expressed in the ovaries of *A. mellifera* queens compared to *A. cerana* queens and is crucial for ovary development. Moreover, *agxt2l* can increase the phospholipid content in ovarian nutrient cells through the glycerophospholipid metabolism pathway to promote embryo formation and is regulated by *brc-z1* (*LOC552255*). These findings suggest that the *brc-z1-agxt2l* signal pathway causes increased egg-laying in the queens of *A. mellifera* compared to the queens of *A. cerana* by accelerating lipid synthesis due to heightened glycerophospholipid metabolism.

Honey bees (genus *Apis*) are highly eusocial insects that have benefited humans for centuries¹. Beekeeping, the culture of both *Apis mellifera* and *Apis cerana*, has been used widely to produce bee products^{2–4} and provide crop pollination⁵. Honey bees also help protect biodiversity⁶ and benefit human health^{7,8}.

The biology of *A. mellifera* has been well studied^{9,10}. Compared to *A. mellifera*, the biology of *A. cerana* in Asia is less studied¹¹ and many questions remain. There are many differences between the two sister species of honey bees. *A. cerana* has smaller body sizes than *A. mellifera*, but is better at collecting sporadic nectar in mountainous or forested areas¹². *A. cerana* also has natural resistance against *Varroa destructor*¹³, better ability to cope with extreme climate¹⁴, and the ability to fight against giant hornets such as *Vespa mandarinia*¹⁵. *A. cerana* does not collect propolis¹⁶ and also fan in their nest entrances in the opposite direction, toward the hive¹⁷ instead of drawing air out by *A. mellifera*. *A. mellifera* has the advantage of higher honey

production, which is the main reason for its spread throughout the world including its introduction to China¹⁸. However, the largest difference, and one that impacts honey yield drastically, is that *A. cerana* has much smaller colonies¹⁹. This is partly because they swarm more often²⁰, partly because their queen egg-laying capability is much lower, compared to that of *A. mellifera*.

The difference in queen egg-laying capacity between the two species is about 4–5 times. *A. mellifera* queens can lay 1500 to 2000 eggs per day^{21–24}, while *A. cerana* queens lay only 420 to 600 eggs per day^{25–27}. There are several possible mechanisms to cause this huge difference. One is that *A. cerana* queens have fewer ovarioles in their ovaries, with only 80–85% of the number in *A. mellifera* queens. However, the difference in ovariole count (across both ovaries) alone cannot fully explain the disparity in egg-laying capacity, because the ratio of ovarioles in queens of *A. mellifera* to *A. cerana* is only about 1.5 to 2.0: *A. mellifera* queens show

¹Honeybee Research Institute, Jiangxi Agricultural University, Nanchang, China. ²Laboratory Animal Science and Technology Center, Jiangxi University of Chinese Medicine, Nanchang, China. ³Jiangxi Province Key Laboratory of Honeybee Biology and Beekeeping, Jiangxi Agricultural University, Nanchang, China. ⁴These authors contributed equally: Luxia Pan, Zilong Wang, Shiqing Zhong. ✉e-mail: bees1965@sina.com

an average of 300 ovarioles²⁸ or a maximum of 400²⁹, while *A. cerana* queens average of 200³⁰. The possibility that *A. mellifera* queens are fed much more often and/or with more or better food compared to *A. cerana* queens is not investigated. While such data do exist for *A. mellifera* queens^{31,32}, comparative data are missing in *A. cerana*. But even if the feeding rates are different, it still would require each ovariole to be more efficient, such that egg production per ovariole would be at least 2.5 times higher in *A. mellifera* than that in *A. cerana*.

We hypothesize that *A. mellifera* queen ovarioles are able to produce mature eggs faster than those of *A. cerana*. This would require differences in physiology, which can be tracked via differences in gene expression. In this study, we used ATAC-seq, RNA-seq, spatial transcriptomics, and cross-species sequence comparisons to compare the gene expression differences in the ovaries of virgin queens and laying queens between the two honey bee species. We identified *agxt2l* as a potential gene: its higher expression in trophocyte cells enhances glycerophospholipid metabolism, thereby accounting for the higher queen egg-laying rate in *Apis mellifera* compared to *A. cerana*.

Results

Difference in queen egg-laying power between *A. mellifera* and *A. cerana*

The number of eggs laid daily by *A. mellifera* queens was significantly higher than those in *A. cerana* ($N = 10$, $Z = -3.82$, $P < 0.01$) (Fig. 1c). Body weight ($N = 10$, $t = 4.32$, $df = 11.39$, $P < 0.01$) (Fig. 1d) and the number of ovarioles ($N = 10$, $t = 16.14$, $df = 18$, $P < 0.01$) (Fig. 1e) in *A. mellifera* queens were significantly higher than those in *A. cerana*. The number of eggs laid per milligram of body weight per day ($N = 10$, $t = 12.11$, $df = 18$, $P < 0.01$) (Fig. 1f) and the number of eggs laid per ovariole per day in *A. mellifera* were significantly higher than those in *A. cerana* ($N = 10$, $t = 20.80$, $df = 18$, $P < 0.01$) (Fig. 1g). Details of statistical analyses are in Supplementary Data 1.

Sequence data quality control

In this study, ATAC-seq and RNA-Seq analyses were conducted for the virgin queens (*A. mellifera*, AmV; *A. cerana*, AcV) and the newly laying

queens (about two months old) (*A. mellifera*, AmQ; *A. cerana*, AcQ). After quality control, each sample obtained an average of 6.52 Gb of clean data (43.48 million clean sequence reads) (Supplementary Data 2). The Q30 values of each sample in the two omics were greater than 90% (Supplementary Data 2). For spatial transcriptome, 2046 spot amounts were detected in the ovaries of *A. mellifera* queen (AmQ). For *A. cerana* queens (AcQ), 1625 spots were detected in the ovaries (Supplementary Data 2). These results showed that sequence quality was acceptable and the bioreplication was reliable.

DEGs between ovaries of *A. mellifera* and *A. cerana* queens

DEGs were identified based on two sets of reference genomes (the reference genomes of *A. mellifera* and *A. cerana*). Pearson correlation coefficients were > 0.95 for all *A. mellifera* bioreplicates using the *A. mellifera* reference genome (Supplementary Fig. 1a), and > 0.91 for all *A. cerana* bioreplicates using the *A. cerana* reference genome (Supplementary Fig. 1b).

Because the reference genomes were different between *A. mellifera* and *A. cerana*, the expression level of the same gene may be different, even if they were the same, if compared using different reference genomes. To avoid this problem, genes showing the same expression trend in a comparison using two reference genomes were selected. In the comparison AmV vs AcV, there were 8481 and 10,315 DEGs using the *A. mellifera* and the *A. cerana* reference genome, respectively (Fig. 2a, d). Among these genes, 5976 genes were homologs (Fig. 2b). Among these homologs, 1154 DEGs showed the same expression trend under the dual species genomes and most of them were up-regulated in the virgin queens (*A. mellifera*, Fig. 2e). In the comparison AmQ vs AcQ, there were 7341 and 9468 DEGs based on these two reference genomes respectively (Fig. 2a, d). Among these genes, 4821 genes were homologs (Fig. 2c). Among these homologs, 1543 DEGs showed the same expression trend in both bee species and most of them were up-regulated in the newly laying queens (*A. cerana*, Fig. 2f).

AmV vs AcV common expression trend DEGs were enriched in Fatty acid degradation, mTOR, Glycerolipid metabolism and other pathways (Supplementary Fig. 2a). AmQ vs AcQ common expression trend DEGs were enriched in Wnt, mTOR, Noth, Glycerophospholipid metabolic pathway, and others (Supplementary Fig. 2b).

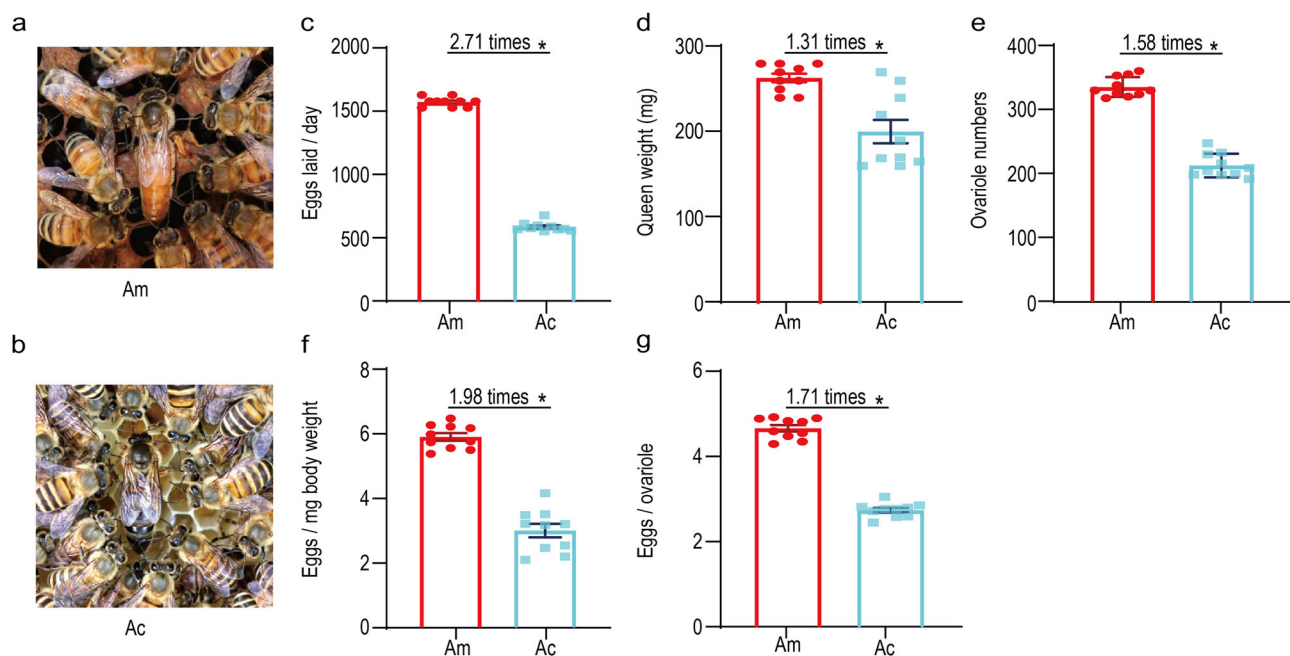


Fig. 1 | Different egg-laying performance of queens in *A. mellifera* and *A. cerana*. **a** The newly laying queen in *A. mellifera* colony. **b** The newly laying queen in *A. cerana* colony. **c** The eggs laid daily of the newly laying queens of *A. mellifera* and *A. cerana*. **d** The body weight of the newly laying queens of *A. mellifera* and *A. cerana*.

e The number of ovarioles in one ovary of *A. mellifera* and *A. cerana*. **f** The number of eggs laid per day per milligram of body weight. **g** The amount of eggs laid per ovariole per day in *A. mellifera* and *A. cerana*.

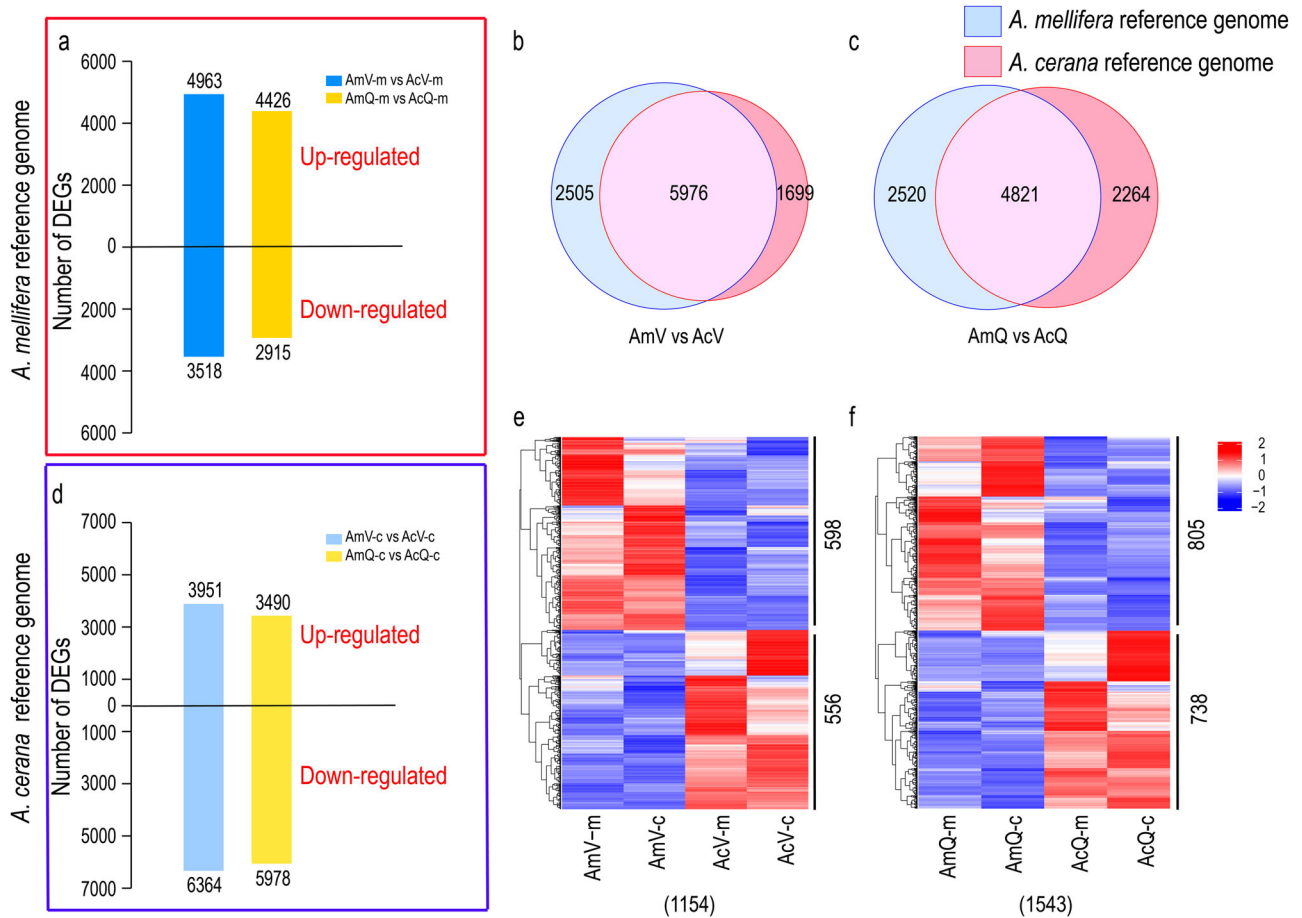


Fig. 2 | Transcriptome data analysis results. **a** The numbers of DEGs and the up-down-regulation relationship in the two comparisons (AmV vs AcV, AmQ vs AcQ) using the *A. mellifera* reference genome. **b** The Venn diagram of overlapped DEGs between AmV vs AcV (using the *A. mellifera* reference genome, AmV-m vs AcV-m) and AmV vs AcV (using the *A. cerana* reference genome, AmV-c vs AcV-c). **c** The Venn diagram of overlapped DEGs between AmQ-m vs AcQ-m and AmQ-c vs

AcQ-c. **d** The numbers of DEGs and the up-down-regulation relationship in the same two comparisons using the *A. cerana* reference genome. **e** The DEGs in AmV vs AcV that showed the same expression trend using either *A. mellifera* or *A. cerana* as a reference genome. **f** The DEGs in AmQ vs AcQ that showed the same expression trend using either *A. mellifera* or *A. cerana* as a reference genome.

Differential open chromatin regions in queen ovaries between the two bee species

To further reveal the distribution of peaks in the genomes, 78,740 and 42,324 peaks in AmV-m (*A. mellifera* virgin queens using the *A. mellifera* reference genome) and AmQ-m (*A. mellifera* laying queens using the *A. mellifera* reference genome) respectively were annotated to the genome of *A. mellifera* (Fig. 3a, b), and there were 22,426 and 17,826 differential peaks in the comparisons AmV-m vs AcV-m and AmQ-m vs AcQ-m (Fig. 3c). While 95,834 and 55,140 peaks in AcV-c (*A. cerana* virgin queens using the *A. cerana* reference genome) and AcQ-c (*A. cerana* laying queens using the *A. cerana* reference genome) respectively were annotated to the genome of *A. cerana* (Fig. 3d, e). The peaks were mainly distributed in the promoter region and intron region, which accounted for more than 54% of the total peaks. There were 19,288 and 15,383 differential peaks in the comparisons AmV-c vs AcV-c and AmQ-c vs AcQ-c (Fig. 3f). There were more up-regulated peaks in *A. mellifera* (AmV, AmQ) under both reference genomes (Fig. 3c, f). The number of differential peaks distributed in intron and promoter regions were predominant (Fig. 3g, h).

Combined analysis of ATAC-Seq and RNA-Seq

When comparing the differential peak-related genes with the DEGs, in AmV vs AcV, there were 6136 overlapped genes between ATAC-Seq and RNA-Seq, when using the *A. mellifera* reference genome. While there were 6604 overlapped genes between ATAC-Seq and RNA-Seq, when using the

A. cerana reference genome. Between these two sets of DEGs, 4411 genes overlapped (Fig. 4a). Analyzing these overlapped genes with the consistent trend genes in Fig. 2e, it was found that 861 differential genes were shared (Fig. 4c). Of them, 88 genes were up-regulated and 84 genes were down-regulated in AmV in both ATAC-seq and RNA-seq under the *A. mellifera* reference genome (Fig. 4e), and the numbers were 131 and 85 under the *A. cerana* reference genome (Fig. 4g). Under the two reference genomes, there were 40 consistently up-regulated genes and 16 consistently down-regulated genes in AmV in both ATAC-seq and RNA-seq (Fig. 4i). AmV vs AcV common trend DEGs were enriched in the fatty acid metabolism pathway and other pathways (Fig. 4j).

In AmQ vs AcQ, there were 5016 and 5599 overlapped genes between ATAC-Seq and RNA-Seq, when using the *A. mellifera* and *A. cerana* reference genomes, respectively. Of these, 3263 DEGs overlapped (Fig. 4b). Analyzing these overlapped genes with the consistent trend genes in Fig. 2f, it was found that 1037 DEGs were shared (Fig. 4d). Of them, 100 genes were up-regulated and 172 genes were down-regulated under *A. mellifera* reference genome (Fig. 4f), and the numbers were 131 up-regulated genes and 127 down-regulated genes in AmQ in both ATAC-seq and RNA-seq under the *A. cerana* reference genome (Fig. 4h). Under the two reference genomes, there were 48 consistently up-regulated and 72 consistently down-regulated genes in AmQ in both ATAC-seq and RNA-seq (Fig. 4i). AmQ vs AcQ common trend DEGs were enriched on Wnt, mTOR and Glycerophospholipid metabolic pathway and other pathways (Fig. 4k).

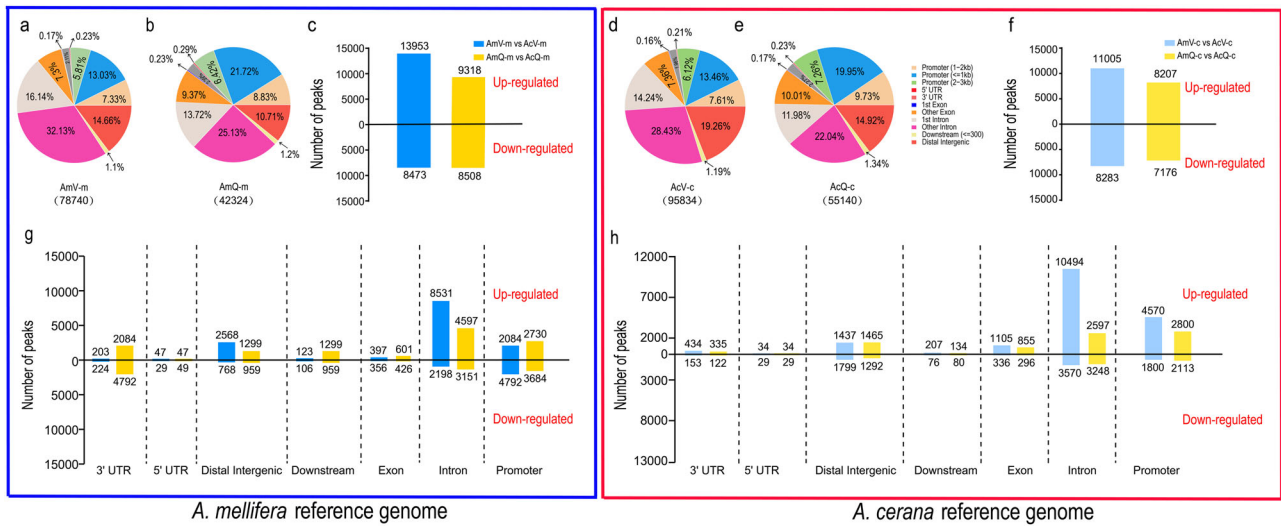


Fig. 3 | ATAC-seq data analysis results. **a, b** The distribution of peaks in AmV and AmQ in the genome of *A. mellifera*. **c** The numbers of differential peaks and the up-down-regulation relationship in the two comparisons (AmV vs AcV, AmQ vs AcQ) using the *A. mellifera* reference genome. **d, e** The distribution of peaks in AcV and AcQ in the genome of *A. cerana*. **f** The number of differential peaks and the up-down-regulation relationship in the same two comparisons using the *A. cerana* reference genome. **g** The distribution of differential peaks in the three comparisons AmV-m vs AcV-m, and AmQ-m vs AcQ-m. **h** The distribution of differential peaks in the three comparisons AmV-c vs AcV-c and AmQ-c vs AcQ-c.

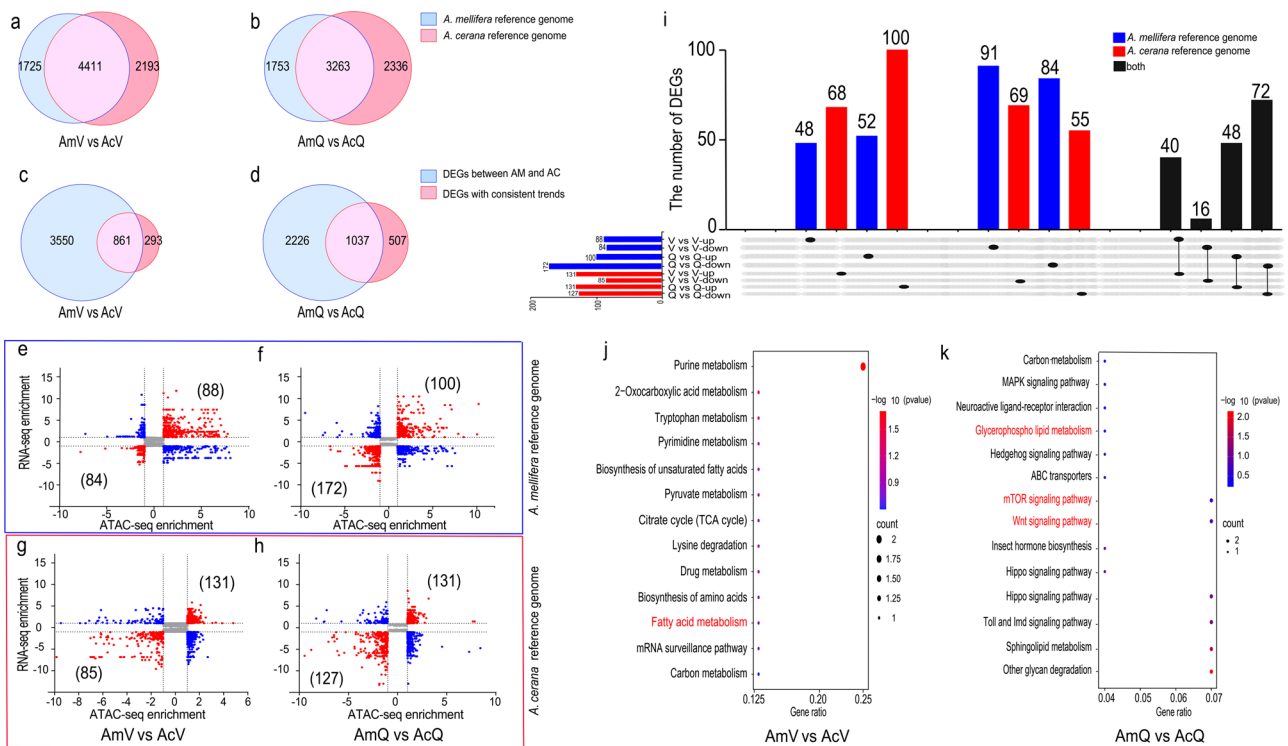


Fig. 4 | Analysis the result of ATAC-Seq and RNA-Seq. **a, b** Venn diagrams of DEGs and differential peak related genes in comparisons AmV vs AcV and AmQ vs AcQ using either *A. mellifera* or *A. cerana* as a reference genome. **c, d** Analyzing the common genes (a, b) with the consistent trend genes in Figs. 2e, f. **e, f** Using the *A. mellifera* reference genome, the RNA-seq and the ATAC-seq common DEGs of all comparison combinations in c, and d were statistically displayed. **g, h** Using the *A. cerana* reference genome, the RNA-seq and the ATAC-seq common DEGs of all comparison combinations in c, and d were statistically displayed. **i** The panels e-h differential genes with the same trend in either reference genomes (the reference genome of *A. mellifera* or *A. cerana*). **j, k** The Kegg pathways of common trend DEGs.

Agxt2l, spr and nedd8 were essential for ovary development

To identify candidate genes that led to differences in queen egg-laying between *A. mellifera* and *A. cerana*, from the 48 consistently up-regulated and 72 consistently down-regulated genes in AmQ vs AcQ in both ATAC-seq and RNA-seq using the dual species genomes, we chose 49 genes that

contained a differential peak in their promoter region (Fig. 5a) as candidates, and found three genes, *agxt2l* (*LOC408817*), *spr* (*LOC725051*) and *nedd8* (*LOC550745*), were essential for ovary development. After RNAi of these three genes, their expression levels (Mann-Whitney U, $P < 0.05$), the number of ovarioles (Mann-Whitney U, $P < 0.05$) and body weight in the

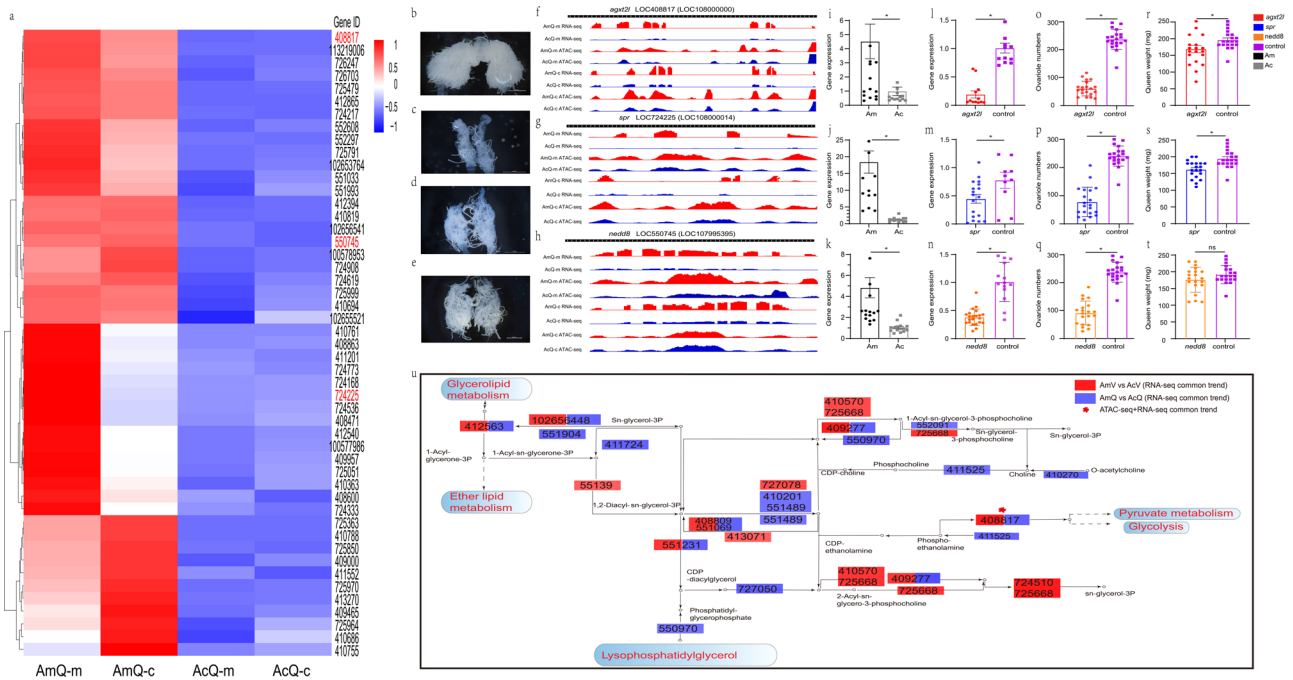


Fig. 5 | Screening and validation of candidate genes. **a** The 49 genes that contain a differential peak in their promoter region. **b–e** Bees ovaries in the control group and RNAi *agxt2l*, *spr* and *nedd8*. **f–h** *agxt2l*, *spr* and *nedd8* differed between AmQ and AcQ in all two omics assays. **i–k** Expression of *agxt2l*, *spr* and *nedd8* in queen ovaries of both species. **l–n** Expression of *agxt2l*, *spr* and *nedd8* in ovaries in RNAi injected queens and control. **o–t** Body weight and number of ovarioles in *A. mellifera* injected

with siRNA of *agxt2l*, *spr*, *nedd8* and the control. **u** The glycerophospholipid metabolic pathway. Genes marked in red represent genes that have differences in gene expression between AmQ and AcQ. (we determined one side ovary because the other side was used for qRT-PCR. But we presented the total number here by timing it by 2 to be consistent with Fig. 1f).

RNAi group (Mann–Whitney *U*, $P < 0.05$ and *T*-test, $P < 0.05$) (Fig. 5i–s) were all significantly reduced compared with the control group, except that the body weight showed no significant changes after RNAi of *nedd8* (*T*-test, $t = -1.78$, $df = 38$, $P > 0.05$) (Fig. 5t) (Supplementary Data 3).

Agxt2l was localized in nutrient cells

Spatial orientation indicated that *A. mellifera* queen ovaries had more cells (nutrient, germ) than that of *A. cerana* queens (Fig. 6a). *agxt2l* was localized in nutrient cells (Fig. 6b) and expressed more in *A. mellifera* queen ovaries than in that of the *A. cerana* queens (Fig. 6c), details in supplementary Fig. 3. The results of DNA template preparation are in Supplementary Fig. 4.

Brc-z1 regulates the transcription of agxt2l gene

To explore the molecular mechanisms leading to the differential expression of the *agxt2l* gene between *A. mellifera* and *A. cerana*, we analyzed the genomic sequences corresponding to the differential peaks located in the promoter region of *agxt2l* in *A. mellifera* and *A. cerana*, and predicted two transcription factors whose binding sites differed between *A. mellifera* and *A. cerana* (Supplementary Fig. 5). To verify these three candidate transcription factors regulating the transcription of *agxt2l*, RNAi was performed in both honey bee species. It was found that after *brc-z1* (*LOC552255*) RNAi, expression level of *brc-z1* ($N = 21$, $Z = -4.49$, $P < 0.05$) (Fig. 7a) and *agxt2l* ($N = 21$, $Z = -2.10$, $P < 0.05$) (Fig. 7b), ovariole number (Mann–Whitney *U*, $Z = -4.98$, $P < 0.05$) (Fig. 7c) and body weight (*T*-test, $t = -2.69$, $df = 38$, $P < 0.05$) (Fig. 7d) of *A. mellifera* queens in the RNAi group, were significantly lower than those in the control group (Supplementary Data 4). While the other genes and *hsf* (list the genes here) had no effect on the transcription of *agxt2l*.

Agxt2l regulates phospholipid content in ovaries

Phospholipid content in larval ovaries of *agxt2l* and *brc-z1* RNAi groups were significantly lower than that of the control group (Kruskal–Wallis,

$H = 48.45$, $P < 0.001$, $P_{adj} < 0.05$), and the phospholipid content in *agxt2l* RNAi group was significantly higher than that in the *brc-z1* RNAi group (Kruskal–Wallis, $H = 48.45$, $P < 0.001$, $P_{adj} < 0.05$) (Fig. 7e) (Supplementary Data 5).

Agxt2l regulates egg-laying performance of queens

The difference in egg-laying number before and after treatment was significantly greater in *agxt2l* RNAi group compared to the control group (*T*-test, $t = 3.24$, $df = 16$, $P < 0.05$) (Fig. 8) (Supplementary Data 7).

Discussion

The principal findings of this study are that we revealed the mechanisms underlying the higher egg-laying capability of *A. mellifera* over *A. cerana*. We identified *agxt2l* as a potential gene: its higher expression in trophocyte cells induces increased glycerophospholipid metabolism, accounting for the higher queen egg-laying rate in *Apis mellifera* compared to *A. cerana*. And *agxt2l* was in turn regulated by *brc-z1* (*LOC552255*) (Figs. 5u, 7, 8, 9, and Supplementary Fig. 5). In addition, *brc-z1* promotes follicular opening. We determined that most of the enrichment pathways in egg-laying queens were related to oviposition or oocyte formation. Finally, we also verified that the egg-laying rate of *A. mellifera* queen is significantly higher than that of *A. cerana* queen, under the same environmental conditions (colony strength, season, and nectar resources).

The egg-laying capability of *A. mellifera* queen and *A. cerana* queen have been studied many times^{33–36} but no study controlled variables which could cause differences besides inherent capability. To rule out contribution due to other factors (such as seasons^{33,35}, population sizes³⁴, regions³⁶, etc.), we tested the egg-laying performance of the two species under the same conditions. We found that the number of eggs laid per milligram of body weight (Fig. 1f) and eggs per ovarioles (Fig. 1g) in *A. mellifera* queen was significantly higher than *A. cerana* queen, we hypothesize that the higher egg-laying rate in *A. mellifera* queen is mainly due to higher efficiency of each ovariole or higher maturation rate of oocytes in each ovariole.

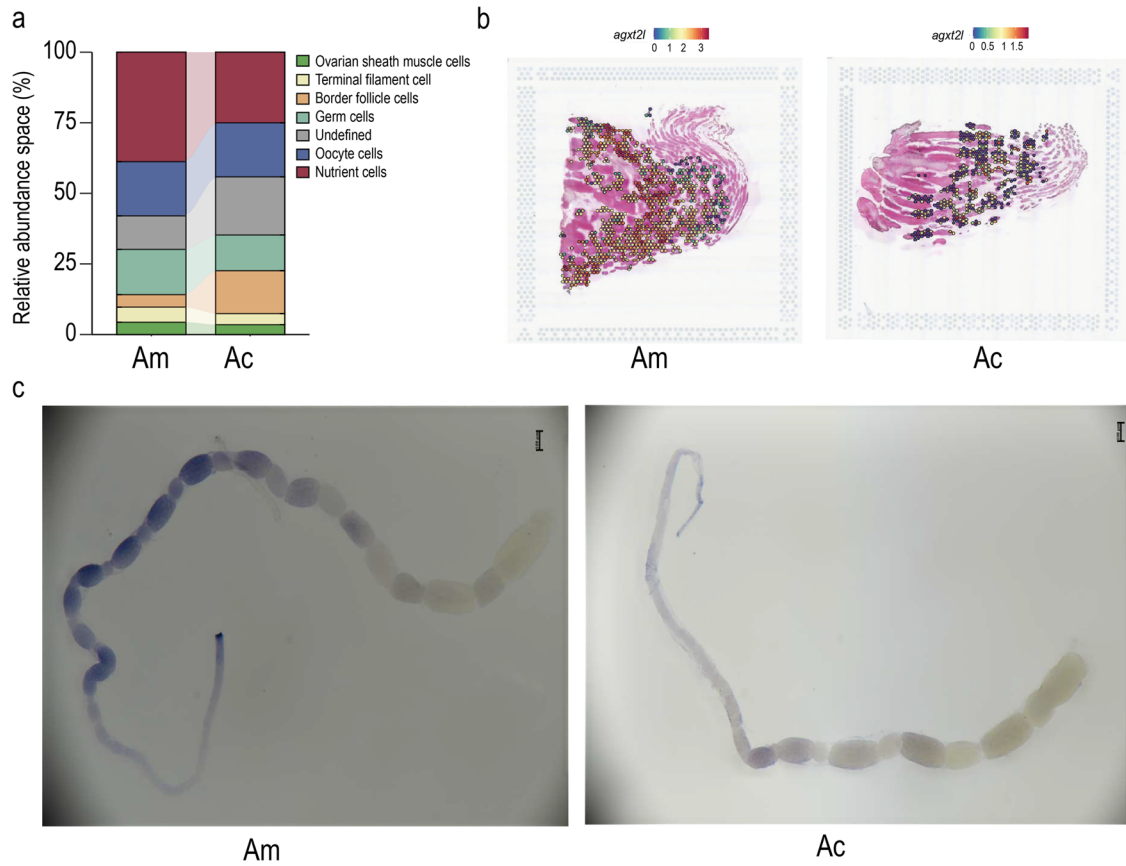
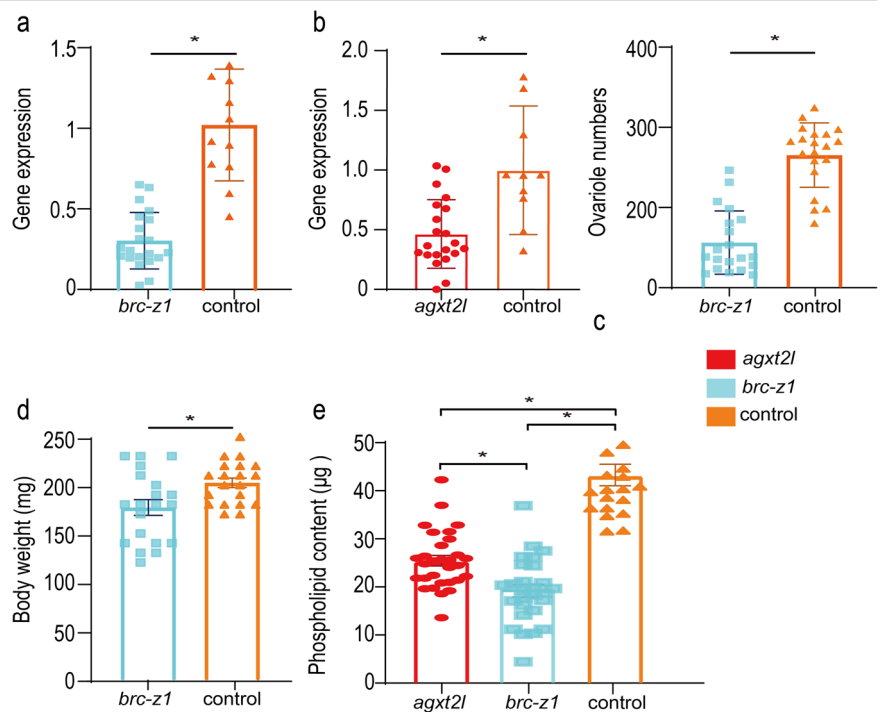


Fig. 6 | Spatial orientation of *agxt2l* expression in ovary. a Cell type and proportion in ovary of *A. mellifera* queen and *A. cerana* queen. **b** Spatial orientation of *agxt2l* expression in ovary. **c** Results of in situ hybridization of *agxt2l*.

Fig. 7 | Motif analysis, transcription factor prediction and change of phospholipid content after RNAi of *agxt2l* and *brc-z1*. a, b Expression of *brc-z1* and *agxt2l* injected with siRNA of *brc-z1*. **c, d** Body weight and number of ovarioles in *A. mellifera* injected with siRNA of *brc-z1*. **e** Change of phospholipid content after RNAi of *agxt2l* and *brc-z1*.



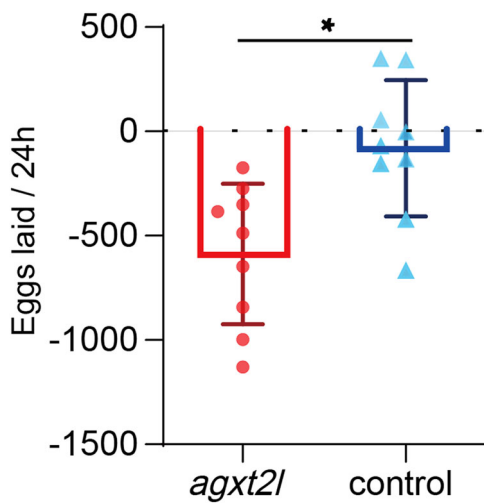


Fig. 8 | *Agxt2l* regulates egg-laying performance of queens. The X-axis shows the experimental (injected *agxt2l*-siRNA solution) and control (injected negative control siRNA solution) groups, while the Y-axis shows the difference obtained by subtracting the pre-interference egg-laying quantity from the post-interference quantity.

The differences in egg-laying rate might be due to differences in glycerophospholipid metabolic rates. In AmV vs AcV, the common trend DEGs were enriched in the fatty acid metabolism pathway (Fig. 5j). This pathway has been shown to play an important role in the development and reproduction of insects^{37–41}. In AmQ vs AcQ, the common trend DEGs were enriched in Wnt, mTOR signaling pathway and Glycerophospholipid metabolic pathway (Fig. 5k). Wnt signaling pathway has been found to be involved in the development of reproductive system, such as follicular development, ovulation, and luteinization⁴². mTOR and glycerolipid metabolism pathways indirectly promote each other. mTOR signaling has been shown to promote reproduction and lifespan in *C. elegans*^{43,44}, female *D. melanogaster*⁴⁵ and female mice⁴⁶. The first step of the Glycerophospholipid metabolic pathway is mediated by mTOR signal transduction⁴⁷, which suggests that Glycerophospholipid metabolic pathway may be related to egg-laying difference between the two species. In addition, in honey bees, approximately 30–40% of the dry weight of an egg is consisted of lipids⁴⁸. Glycerophospholipids are important lipid components in the queen ovaries and play crucial roles in the membrane structure and cell functions⁴⁹, which suggests that glycerophospholipid metabolic rate is the reason for the difference in egg-laying rate.

Agxt2l, *spr* and *nedd8* promotes ovary development. We found that *agxt2l*, *spr* and *nedd8* were expressed higher in *A. mellifera* queen than in *A. cerana*, and they enhanced queen ovary development (Fig. 5c–e). Previous studies indicated that *spr* enhances egg-laying and female fecundity in *Bactrocera dorsalis* (Diptera: Tephritidae)⁵⁰, *D. melanogaster*⁵¹ and *Spodoptera litura*⁵². Zebrafish *nedd8* facilitates ovarian development and the maintenance of female secondary sexual characteristics via suppression of androgen receptor activity⁵³. This suggests that in honey bees, *agxt2l*, *spr* and *nedd8* gene may be the candidate genes involved in differential egg-laying capacity between the two sister species.

The rate of glycerophospholipid metabolic is promoted by *agxt2l*, which itself is enhanced by *brc-z1*. *agxt2l* is located in glycerophospholipid metabolic pathway and belongs to a subfamily of proteins called “Class II transaminases”, and is a modulator of phospholipid metabolism⁵⁴. Liang et al. found that phospholipids promote ovarian development in shrimps⁵⁵. In addition, in pregnant rabbits⁵⁶, pigs⁵⁷ and sheep⁵⁸, phospholipids in the ovaries reach high levels during ovulation and the levels are maintained throughout pregnancy. These results indicate that phospholipids are related not only to ovarian development but also to embryo formation. We found that *brc-z1* bound to the *agxt2l* promoter region (in both *A. mellifera* and *A. cerana*.) and positively regulated *agxt2l*. The broad-complex (*br-c*) is an

early ecdysone hormone response gene that encodes four zinc finger protein subtypes (Z1, Z2, Z3, and Z4). In *Blattella germanica*, these four zinc finger isomers all play an important role in embryogenesis⁵⁹. When BR-C is mis-expressed, the follicular cells in the front of the oocyte do not migrate forward properly⁶⁰. In *D. melanogaster*, *brc-z1* is involved in the formation of egg and ovum^{61–63} and is specifically expressed in nurse cells, somatic follicle cells⁶⁴, and egg chamber⁶⁵ which indicate that *brc-z1* not only regulates *agxt2l* but also affects ovary development.

Increased glycerophospholipid metabolism due to higher expression of *agxt2l* in trophocyte cell explains the higher egg-laying rate in *A. mellifera* queens. We found that *agxt2l* is highly expressed in trophoblast cells (Fig. 6b) and the proportion of trophoblast cells in *A. mellifera* queens is higher than that in *A. cerana*. In bees, trophoblast cells contain a large number of coarse endoplasmic reticulum and Golgi cytoplasm, mitochondria, lipids, carbohydrates and proteins^{65–68}. The presence of these organelles indicates that trophoblast cells are capable of synthesizing, absorbing, metabolizing, and storing substances, especially those derived from hemolymph⁶⁹. After interfering with *agxt2l*, glycerophospholipid metabolism of trophoblast cells was limited, and lipid synthesis/ transport was decreased (Fig. 9), thus perhaps resulting a delay (or reduction) in egg formation. Based on the present results, we provide evidence that the rate of lipid synthesis controlled by *agxt2l* is the main reason why the *A. mellifera* queens have higher egg-laying capability than the *A. cerana* queens.

Furthermore, evolutionary pressure disparities likely underlie the variation in reproductive phenotypes. *Apis mellifera ligustica* is native to the Apennine Peninsula in the central Mediterranean, and *Apis cerana cerana* is mainly distributed in the subtropical humid area of the southern Longnan River Valley, the warm temperate humid area of the northern Longnan, the temperate semi-humid area of the southern Longzhong, and the temperate semi-arid area of the northern Longzhong, east of the Wushaoling Mountains in China. The monsoon climate in China, compared to Mediterranean climates, is characterized by high diversity, more acute changes, and a more scattered nectar flow. There are also large differences among different regions in China. All of these factors favor the phenotype for more flexible reproduction to achieve better resource management and faster responses to changing environments (including swarming and absconding), which increases the chance of survival for the colony under a changeable climate.

Materials and methods

Queen egg-laying capacity

A. mellifera ligustica colonies (Jiangxi Agricultural University, 28.46°N, 115.49°E, Nanchang, China) and *A. cerana cerana* colonies (Yifeng County, 28.26°N, 114.39°E, Jiangxi, China) ($N = 10$ each species) with newly laying queens (approximately 2 months old) were randomly selected for this experiment. The distance between the two places is 144 km. The queen of each colony was restricted to laying eggs on a comb for 24 h. The number of eggs on the comb was counted by taking digital photos (Canon EOD 70D) and using Image J (v1.54 d). This egg-laying experiment was repeated twice. We then fixed the queens on wax dish ($N = 10$ for each species) and dissected the ovaries. Ovary sections were prepared according to the method reported by Yi et al.⁷⁰. Then, the number of ovarioles from both ovaries was counted under a dissection microscope (40x Nikon DS. Fi3). The differences in egg number and ovariole number between the two species were analyzed using Mann–Whitney Test and *T*-test in SPSS Statistics version 25.0.

Insects and sample collection

A. mellifera ligustica colonies and *A. cerana cerana* colonies ($N = 14$ colonies each species) in Jiangxi Agricultural University (28.46°N, 115.49°E), Nanchang, China, were used in the rest of this study. For *A. mellifera*, the queen of each colony was confined on a comb to lay eggs for six hours (8:00 am–2:00 pm), and then the queen was separated from the experimental comb using a queen excluder. After egg hatching, the larvae were transferred to queen cells. On the tenth day after hatching, twelve queenless colonies were

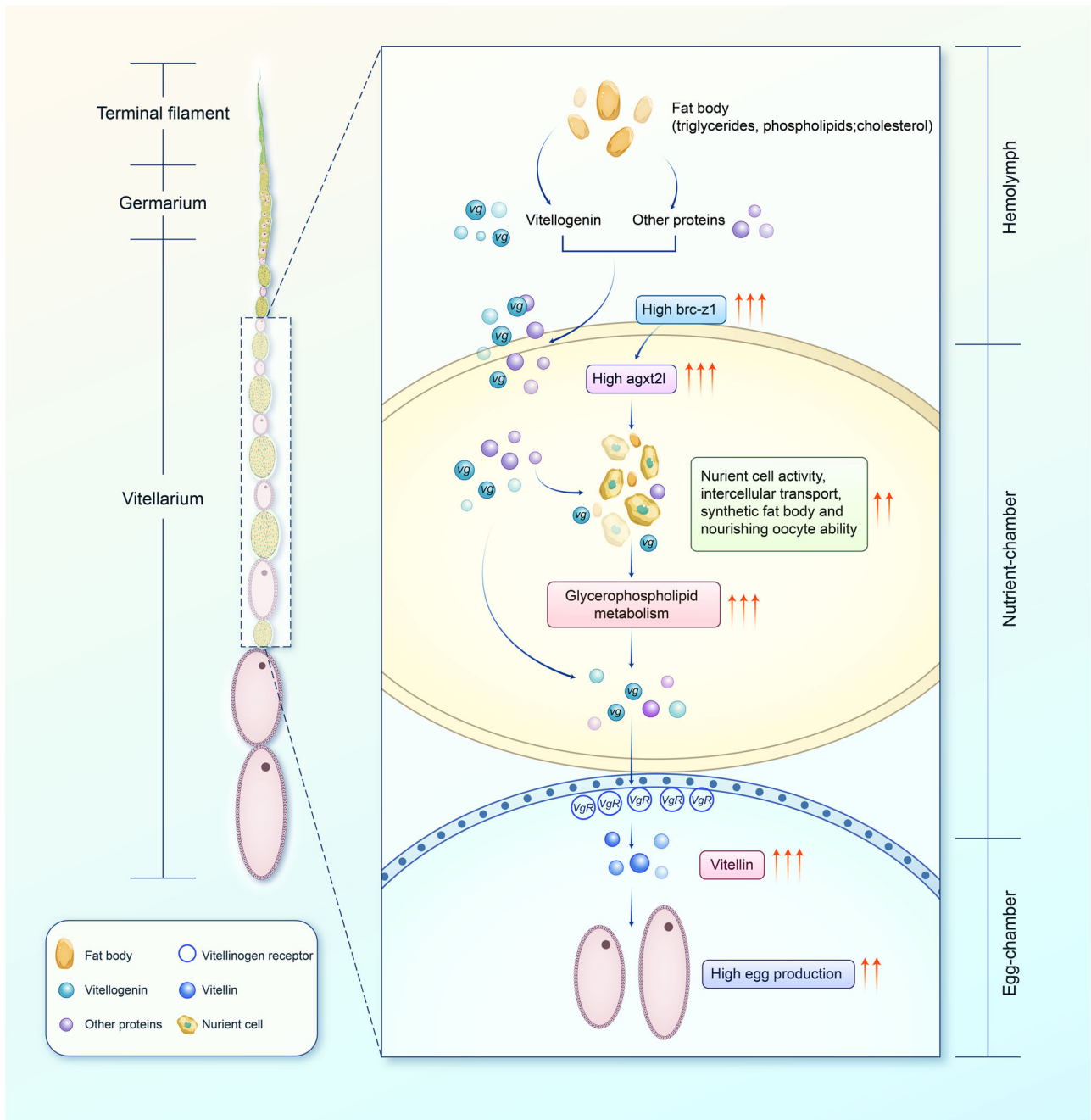


Fig. 9 | Increased glycerophospholipid metabolism due to higher expression of *agxt2l* in trophocyte cell explains the higher queen egg laying rate in *Apis mellifera* than *A. cerana*.

prepared as nucleus colonies. In the afternoon of the 11th day, some queen cells were placed in the queenless colonies to obtain laying queens, and some were placed in queen cages to obtain virgin queen samples. Seven ovary samples of the newly emerged virgin queen were collected. After the queens had mated, seven ovary samples of the newly laying queens (approximately two months old) were collected. The sampling methods of *A. cerana* were the same as *A. mellifera*.

A total of 28 pairs of ovaries were collected from four types of queens, these were virgin queens and newly laying queens of both bee species ($N = 7$ for each type).

RNA extraction, transcriptome sequencing, and data analysis

Total RNAs were extracted from the ovary samples using Trizol Reagent (Ambion/Invitrogen, USA). RNA integrity and total amount were detected

by Agilent 2100 Bioanalyzer (Agilent Technologies, CA, USA). All RNA samples that passed quality control were used to construct the library⁷¹. The library preparations were sequenced on an Illumina Novaseq platform (performed by Novogene Co., Ltd. (Beijing, China) and 150 bp paired-end reads were generated. From the sequencing data, reads containing just adapters and undetermined bases as well as low-quality reads (Qphred \leq 20 reads with more than 50% of the total read length) were filtered out.

The cleaned reads were aligned to the *A. mellifera* genome version Amel_HAV3.1(ftp.ncbi.nlm.nih.gov/genomes/all/GCF/003/254/395/GCF_003254395.2_Amel_HAV3.1/) or to the *A. cerana* reference genome (ftp://ftp.ncbi.nlm.nih.gov/assembly/GCA_020141525.1) using HISAT2 software⁷². The expression level was calculated by Fragments Per Kilobase of transcript per Million (FPKM) base pairs, with standardized annotation of the length of the transcript and the total number of reads aligned with the

transcriptome. Analysis of differential expression was performed using the DESeq2 R package (1.32.0). The p-value was corrected for multiple comparisons with a false discovery rate (FDR) < 0.05^{73–75}. Genes with padj ≤ 0.05 were defined as differentially expressed genes.

After that, all DEGs were mapped to the Gene ontology (GO) database for enrichment analysis of functional significance. Finally, pathway enrichment analysis was performed in the Kyoto Encyclopedia of Genes and Genomes (KEGG) database⁷⁶.

Nuclear extraction, ATAC-seq, and data analyses

The ATAC-seq was performed according to Buenrostro et al.^{77–79} and performed by Novogene Co., Ltd. (Beijing, China). Cell nuclei were extracted from the ovary samples and the nuclei particles were re-suspended in the Tn5 transposase reaction mixture. The transposition reaction was incubated at 37 °C for 30 min. After transposition of Novogene, equimolar adapter1 and adapter2 were added to amplify the library by PCR. Then, the PCR products were purified by AMPure beads, and the quality of the libraries was evaluated by Qubit. The libraries were sequenced on an Illumina Novaseq platform.

Index of the reference genome was built using BWA (v0.7.12) and clean reads were aligned to the reference genome using BWA mem, by default parameters. Peaks with q-value threshold of 0.05 were used for all data sets, peak-related genes were identified and annotated by ChIPseeker⁸⁰. The peaks with fold change more than 2(|log₂fc| > 1) were considered as differential peaks.

Genome homology alignment and data analyses

The homologs between *A. mellifera* and *A. cerana* were identified using Blast software (2.2.26) with *e* value < 1e−10. In the process of RNA-seq and ATAC-seq analyses, the homologous genes with the same trend were selected, and the differential genes and differential peaks showing difference when using the two sets of genomes as references were eliminated to avoid differences caused by different reference genomes. The analytical technique route was shown in Supplementary Fig. 6.

Larval RNAi

The queen of a colony was confined on a comb to lay eggs for six hours, and then the queen was separated from the experimental comb by a queen excluder. After hatching of the eggs, the larvae were transferred to 24-cell tissue culture plates containing 150 μL artificial food, and then incubated at 35 °C and 85 relative humidity (RH). Each larva was fed with 150 μL artificial food two times daily. The vitro larval rearing method followed Schmehl et al.⁸¹. The queen food formula consisted of 53% fresh bee royal jelly, 6% glucose, 6% fructose, 1% yeast extract, and 34% distilled water⁸². When the larvae reached 2.5-day-old they were randomly divided into two groups; one group was injected with about 1 μL RNAi solution (2 μg/μL), another group was injected with 1 μL negative control siRNA. Injection was performed by an Eppendorf FemtoJet 4i with an injecting needle at 1 μm in size, injection pressure at 500 hpa, and Output pressure (PC) at 15 hpa. Survival after injection was between 70–80%. For RNAi of *agxt2l*, *spr*, and *nedd8*, 24 larvae's ovaries were randomly collected 48 h later after injection to determine RNAi efficiency using qRT-PCR. The remaining larvae were further reared until they became adult bees (the queens were virgins at the time of sampling). The body weight and ovarian tubes of the newly emerged bees were measured. When we injected siRNA of *brc-z1* to test the relationship between *brc-z1* and *agxt2l*, 33 larvae's ovaries were randomly collected 48 h after injection to determine RNAi efficiency using qRT-PCR. The siRNA sequences are shown in Supplementary Data 6.

RNAi of egg-laying queen

A. mellifera ligustica colonies (*N* = 10) in Jiangxi Agricultural University (28.46°N, 115.49°E), Nanchang, China, were used in this study. All colonies had similar population sizes, and each contained a newly laying queens (approximately 2 months old). Queens with similar 24-hour egg-laying capacities (measured over three consecutive days) were selected (*N* = 6) and

randomly divided into two groups (*n* = 3 per group). One group (*n* = 3) was injected with about 3 μL *agxt2l*-siRNA solution (1 μg/μL), another group (*n* = 3) was injected with 3 μL negative control siRNA (1 μg/μL). RNAi in egg-laying queens was performed following the method reported by Han et al.⁸³. Prior to injection, queens were transferred to the laboratory and anesthetized with CO₂. Injections were performed dorsally between the second and third abdominal segments using an Eppendorf FemtoJet 4i with injecting needle at 3 μm in size, with an injection pressure at 70 hPa and output pressure (PC) at 15 hPa. Injected queens were given time to recover and placed back into their original colonies. 12 h post-injection, the egg-laying capacity of each queen was quantified. The impact of the treatment and control groups on queen fecundity was assessed by comparing the difference in egg numbers before and after RNAi injection.

Quantitative real-time PCR (qRT-PCR)

Total RNA was extracted from ovary samples using Trizol Reagent (Ambion/Invitrogen, USA) and RNA integrity was detected by agarose gel electrophoresis. RNA concentration and purity (OD_{260/280} value) were measured by an ultraviolet spectrophotometer. The RNA samples (1 μg/μL) were reverse transcribed into cDNA using the PrimeScript™ RT reagent Kit (Takara, Japan). The *gapdh* and *β-actin* gene were used as internal reference. The primer sequences are shown in Supplementary Data 6. qRT-PCR was performed according to Pan et al.⁸⁴. Vandesompele's method was used to analyze qRT-PCR data⁸⁵.

Detection of insect phospholipid by ELISA

Larval ovaries were used in this experiment to detect the phospholipid content using the Shanghai Meilian Insect Phospholipid Enzyme-Linked Immunosorbent Assay Kit. The larval ovary samples were weighed at first and then were homogenized (homogenate proportion of 10%, that is, 1 milligram tissue plus 9 ml of PBS). Then, 78 larvae ovary samples (control group=21, *agxt2l* RNAi group=30 and *brc-z1* RNAi group=27) were centrifuged for about 20 min (14,000 RPM) to collect the supernatant. Subsequently, the absorbance (OD value) of each supernatant was measured by BioTek Synergy_HTX Multimode Reader (BioTek Synergy HTX, Bio-TEK) at 450 nm wavelength, and the sample concentration was calculated.

Spatial transcriptomics

One ovary of egg-laying queen of *A. mellifera* or *A. cerana* was used as a sample. After the sample was embedded with OTC, tissue permeation was performed. The optimal permeation time (30 min) was selected, and RT Master Mix was added into the permeated tissue section for amplification. Finally, fragment screening was performed to obtain cDNA library. Transcriptome sequencing was performed by LC-Bio Technology Co., Ltd (Hangzhou, China). The original data underwent data filtering, comparison and quantification to obtain the gene expression matrix of spots using the official analysis software of 10x Genomics (<https://support.10xgenomics.com/spatial-gene-expression/software/overview/welcome>). Seurat⁸⁶ was used for difference analysis and visual analysis.

in situ hybridization

For in situ detection of the *agxt2l*, sense and antisense probes were synthesized using *agxt2l* specific primers with a T7 promoter sequence at the 5'-ends (*Agxt2l-Fow1*: 5'-TAATACGACTCACTATAGGGCGATGCTCTGTTGGTGGGCAAATTCTAC-3'; *Agxt2l-Rev1*: 5'-TAATACGACTCACTATAGGGCGACCATAGGTTTACCTACAGTGACTATATCC-3') in combination with primers lacking the T7 sequence (*Agxt2l-Fow2*: 5'-TGCTGTGGTGGGCAAATTCTAC-3'; *Agxt2l-Rev2*: 5'-CCATAGGTTCCTACAGTGACTATATCC-3'). These primers generated a product of 223 bp. The antisense and sense products were produced by the primer combination *Agxt2l-Fow2*+*Agxt2l-Rev1* and *Agxt2l-Fow1*+*Agxt2l-Rev2*, respectively. Amplification conditions were: 94 °C for 2 min, 10 cycles of 94 °C for 15 s, 55 °C for 30 s, 72 °C for 45 s and 20 cycles of 94 °C for 15 s, 55 °C for 30 s, 72 °C for 45 s (+5 s per cycle), final extension step at 72 °C for 7 min, 4 °C, ∞.

Aliquots of the amplification products were checked on agarose gels and quantified spectrophotometrically. RNA probes were generated by *in vitro* transcription from the T7 promoter using the DIG RNA Labeling Kit (SP6/T7) (Roche Applied Science). Fixation of dissected ovary and the subsequent hybridization and detection reactions were performed following the protocol optimized by Osborne and Dearden⁸⁷ for *in situ* hybridization studies on honey bees.

Statistics and reproducibility

Data statistical analyzes were performed using SPSS Statistics software version 25.0 (IBM Corp., Armonk, NY) or GraphPad Prism version 8 for Windows (GraphPad Software, San Diego, CA, USA). The Mann–Whitney *U*-test, the *T*-test, and the Kruskal–Wallis in SPSS Statistics version 25.0 were used to evaluate queen egg-laying capacity (Figs. 1c–g, 7c, d), changes of phospholipid content after RNAi of *agxt2l* and *brc-z1* (Fig. 7e), egg-laying performance before and after RNAi treatment (Fig. 8), and qPCR results throughout the text (Figs. 5i–t, 7a, b).

Data availability

The ATAC-seq and RNA-seq data generated in this study are available in the database of the National Center for Biotechnology Information (NCBI). For the *A. mellifera* samples, the RNA-seq data retrieval number is PRJNA1015187, ATAC-seq data retrieval number is PRJNA1015357; For the *A. cerana* samples, the RNA-seq data retrieval number is PRJNA1015354, ATAC-seq data retrieval number is PRJNA1015364. Source data underlying graphs in the manuscript can be found in the Supplementary Data 1 file.

Received: 13 January 2025; Accepted: 14 July 2025;

Published online: 23 July 2025

References

- Crane, E. Honey. *A Comprehensive Survey* (Heinemann, 1975).
- ZHAO, Y. -z. et al. Differential volatile organic compounds in royal jelly associated with different nectar plants. *J. Integr. Agric.* **15**, 1157–1165 (2016).
- Pascoe, C. D. et al. Gene expression analysis in asthma using a targeted multiplex array. *BMC Pulm. Med.* **17**, 1–14 (2017).
- Collazo, N. et al. Health promoting properties of bee royal jelly: food of the queens. *Nutrients* **13**, 543 (2021).
- Parker, R. et al. Ecological adaptation of diverse honey bee (*Apis mellifera*) populations. *PLoS One* **5**, e11096 (2010).
- Orr, M. C. et al. Global patterns and drivers of bee distribution. *Curr. Biol.* **31**, 451–458. e454 (2021).
- AU-IBAR. The Inaugural report on the status of apiculture in Africa 2019: Opportunities and strategies for development of the sector. (Africa Union Inter African Bureau for Animal Resources, 2019).
- Durazzo, A. et al. Bee products: a representation of biodiversity, sustainability, and health. *Life* **11**, 970 (2021).
- Winston, M. L. *The Biology of the Honey Bee* (Harvard University Press, 1987).
- Wang, M. et al. RNA m⁶A modification functions in larval development and caste differentiation in honeybee (*Apis mellifera*). *Cell Rep.* **34**, 108580 (2021).
- Hepburn, H. R. & Radloff, S. E. *Honeybees of Asia* (Springer Science & Business Media, 2011).
- Cheng, S. *Special Management of Apis cerana cerana*. Vol. 1 (China Agriculture Press, 2001).
- Peng, Y.-S., Fang, Y., Xu, S. & Ge, L. The resistance mechanism of the Asian honey bee, *Apis cerana* Fabr., to an ectoparasitic mite, *Varroa jacobsoni* Oudemans. *J. Invertebr. Pathol.* **49**, 54–60 (1987).
- Tan, K. et al. An 'I see you' prey–predator signal between the Asian honeybee, *Apis cerana*, and the hornet, *Vespa velutina*. *Anim. Behav.* **83**, 879–882 (2012).
- Carreck, N. How does *Apis cerana* defend itself against hornets?. *Bee World* **90**, 64–65 (2013).
- Crane, E. *Bees and Beekeeping: Science, Practice and World Resources*. (Heinemann Newness, 1990).
- Hall, K. *Spatial Aspects of Foraging Behaviour in Eastern Honeybees, Apis cerana* (University of Exeter, 2017).
- Yang, G. Harm of introducing the western honeybee *Apis mellifera* L. to the Chinese honeybee *Apis cerana* F. and its ecological impact. *Acta Entomol. Sin.* **48**, 401 (2005).
- Theisen–Jones, H. & Bienefeld, K. The Asian honey bee (*Apis cerana*) is significantly in decline. *Bee World* **93**, 90–97 (2016).
- Koetz, A. The Asian honey bee (*Apis cerana*) and its strains—with special focus on *Apis cerana* Java genotype. (ed Fisheries Department of Agriculture, and Forestry, State of Queensland, Australia, 58p) (2013).
- Snodgrass, R. E. *Anatomy of the Honey Bee* (Cornell University Press, 1956).
- Page, R. & Erickson, E. Reproduction by worker honey bees (*Apis mellifera* L.). *Behav. Ecol. Sociobiol.* **23**, 117–126 (1988).
- Tarpy, D. & Mayer, M. The effects of size and reproductive quality on the outcomes of duels between honey bee queens (*Apis mellifera* L.). *Ethol. Ecol. Evol.* **21**, 147–153 (2009).
- Kumar, N. Evaluation of larval grafted queen and natural reared queen of Italian honey bees (*Apis mellifera* L.). *J. Pharmacogn. Phytochem.* **7**, 3181–3183 (2018).
- Kapil, R. The length of life and the brood-rearing cycle of the Indian bee. *Bee World* **38**, 258–263 (1957).
- Ruttner, F. *Biogeography and Taxonomy of Honeybees* (Springer Science & Business Media, 2013).
- Hoan, N. D. & Hoan, P. D. Factor effects on number of eggs laid of queen bee species *Apis cerana* at Northeastern region of Vietnam. *Livest. Res. Rural Dev.* **33**, 1–9 (2021).
- Ozbakir, G. O. Effects of rearing method on some morphological and reproductive organ characteristics of queen honey bees (*Apis mellifera* L.). *Med. Weter.* **77**, 89–94 (2021).
- Jackson, J. T., Tarpy, D. R. & Fahrback, S. E. Histological estimates of ovariole number in honey bee queens, *Apis mellifera*, reveal lack of correlation with other queen quality measures. *J. Insect Sci.* **11**, 82 (2011).
- Zhong, W.-L., Ding, G.-L., Yuan, C.-Y., Huang, J.-X. & Feng, M. Honey bee (*Apis cerana*) queen rearing methods influence queen morphological characteristics and reproductive related gene expression. *Apidologie* **55**, 1–13 (2024).
- Lindauer, M. Ein Beitrag zur frage der arbeitsteilung im bienenstaat. *Z. Vgl. Physiol.* **34**, 299–345 (1952).
- Haydak, M. H. Honey bee nutrition. *Annu. Rev. Entomol.* **15**, 143–156 (1970).
- Bodenheimer, F. S. Studies in animal populations. II. Seasonal population-trends of the honey-bee. *Q. Rev. Biol.* **12**, 406–425 (1937).
- Free, J. & Williams, I. H. The influence of a honeybee (*Apis mellifera*) colony on egg-laying by its queen. *Entomol. Exp. Appl.* **15**, 224–228 (1972).
- Shehata, S., Townsend, G. & Shuel, R. Seasonal physiological changes in queen and worker honeybees. *J. Apic. Res.* **20**, 69–78 (1981).
- Hatjina, F. et al. A review of methods used in some European countries for assessing the quality of honey bee queens through their physical characters and the performance of their colonies. *J. Apic. Res.* **53**, 337–363 (2014).
- Chertemps, T. et al. A female-biased expressed elongase involved in long-chain hydrocarbon biosynthesis and courtship behavior in *Drosophila melanogaster*. *Proc. Natl Acad. Sci. U.S.A.* **104**, 4273–4278 (2007).
- Alabaster, A. et al. Deficiencies in acetyl-CoA carboxylase and fatty acid synthase 1 differentially affect eggshell formation and blood meal

- digestion in *Aedes aegypti*. *Insect Biochem. Mol. Biol.* **41**, 946–955 (2011).
39. Hagström, ÅK., Lienard, M. A., Groot, A. T., Hedenström, E. & Löfstedt, C. Semi-selective fatty acyl reductases from four heliothine moths influence the specific pheromone composition. *PLoS One* **7**, e37230 (2012).
 40. Li, L. et al. Jinglyngangmycin increases fecundity of the brown planthopper, *Nilaparvata lugens* (Stål) via fatty acid synthase gene expression. *J. Proteom.* **130**, 140–149 (2016).
 41. Zheng, T., Qian, Y. & Zhang, D. Research progress on key genes of fatty acid synthesis pathway in insects. *Chin. Biotech.* **37**, 19–27 (2017).
 42. Xiaoyang, S. & Yanling, W. Wnt signaling pathways in mammalian reproduction. *Prog. Biochem. Biophys.* **30**, 180–184 (2003).
 43. Vellai, T. et al. Influence of TOR kinase on lifespan in *C. elegans*. *Nature* **426**, 620–620 (2003).
 44. Pan, K. Z. et al. Inhibition of mRNA translation extends lifespan in *Caenorhabditis elegans*. *Aging Cell* **6**, 111–119 (2007).
 45. LaFever, L., Feoktistov, A., Hsu, H.-J. & Drummond-Barbosa, D. Specific roles of target of rapamycin in the control of stem cells and their progeny in the *Drosophila* ovary. *Development* **137**, 2117–2126 (2010).
 46. Zhang, H. et al. Somatic cells initiate primordial follicle activation and govern the development of dormant oocytes in mice. *Curr. Biol.* **24**, 2501–2508 (2014).
 47. Dolce, V., Rita Cappello, A., Lappano, R. & Maggiolini, M. Glycerophospholipid synthesis as a novel drug target against cancer. *Curr. Mol. Pharmacol.* **4**, 167–175 (2011).
 48. Ziegler, R. & Van Antwerpen, R. Lipid uptake by insect oocytes. *Insect Biochem. Mol. Biol.* **36**, 264–272 (2006).
 49. Zhao, H., Mashilingi, S. K., Liu, Y. & An, J. Factors influencing the reproductive ability of male bees: current knowledge and further directions. *Insects* **12**, 529 (2021).
 50. Chen, H. et al. CRISPR/Cas9-induced mutation of sex peptide receptor gene *bdspr* affects ovary, egg laying, and female fecundity in *Bactrocera dorsalis* (Hendel)(Diptera: Tephritidae). *J. Insect Sci.* **23**, 2 (2023).
 51. Yapici, N., Kim, Y.-J., Ribeiro, C. & Dickson, B. J. A receptor that mediates the post-mating switch in *Drosophila* reproductive behaviour. *Nature* **451**, 33–37 (2008).
 52. Li, C. et al. Molecular characterization and functional analysis of a putative sex-peptide receptor in the tobacco cutworm *Spodoptera litura* (Fabricius, 1775)(Lepidoptera: Noctuidae). *Aust. Entomol.* **53**, 424–431 (2014).
 53. Yu, G. et al. Zebrafish Nedd8 facilitates ovarian development and the maintenance of female secondary sexual characteristics via suppression of androgen receptor activity. *Development* **147**, dev194886 (2020).
 54. Deng, Y., Wu, L., Ding, Q. & Yu, H. AGXT2L1 is downregulated in carcinomas of the digestive system. *Oncol. Lett.* **20**, 1318–1326 (2020).
 55. Liang, X. et al. Effects and mechanism of different phospholipid diets on ovary development in female broodstock Pacific white shrimp, *Litopenaeus vannamei*. *Front. Nutr.* **9**, 830934 (2022).
 56. MORIN, R. J. Ovarian phospholipid composition and incorporation of [¹⁴C] acetate into the phospholipid fatty acids of ovaries from non-pregnant and pregnant rabbits. *Reproduction* **17**, 111–117 (1968).
 57. Boyd, E. M. The relation of lipid composition to physiological activity in the ovaries of pregnant and pseudopregnant rabbits. *J. Biol. Chem.* **108**, 607–617 (1935).
 58. Bloor, W., Okey, R. & Corner, G. W. The relation of the lipids to physiological activity: I. The changes in the lipid content of the corpus luteum of the sow. *J. Biol. Chem.* **86**, 291–306 (1930).
 59. Piulachs, M.-D., Pagone, V. & Bellés, X. Key roles of the *Broad-Complex* gene in insect embryogenesis. *Insect Biochem. Mol. Biol.* **40**, 468–475 (2010).
 60. Tzolovsky, G., Deng, W.-M., Schlitt, T. & Bownes, M. The function of the *broad-complex* during *Drosophila melanogaster* oogenesis. *Genetics* **153**, 1371–1383 (1999).
 61. Slack, F. & Ruvkun, G. Temporal pattern formation by heterochronic genes. *Annu. Rev. Genet.* **31**, 611–634 (1997).
 62. Dobens, L. L. & Raftery, L. A. Integration of epithelial patterning and morphogenesis in *Drosophila* ovarian follicle cells. *Dev. Dyn.* **218**, 80–93 (2000).
 63. Wilson, T. G., Yerushalmi, Y., Donnell, D. M. & Restifo, L. L. Interaction between hormonal signaling pathways in *Drosophila melanogaster* as revealed by genetic interaction between *Methoprene-tolerant* and *Broad-Complex*. *Genetics* **172**, 253–264 (2006).
 64. Terashima, J. & Bownes, M. *E75A* and *E75B* have opposite effects on the apoptosis/development choice of the *Drosophila* egg chamber. *Cell Death Differ.* **13**, 454–464 (2006).
 65. Locke, M. in *Insect ultrastructure* (ed King R. C., Akai H.) 151–197 (Plenum, 1984).
 66. Cruz-Landim, C. Modificações das células do corpo gorduroso de rainhas de *Apis mellifera* L.(Hymenoptera, Apidae). *Cienc. Cult.* **37**, 471–475 (1985).
 67. Dean, R., Locke, M., Collins, J., Kerkut, G. & Gilbert, L. in *Comparative insect physiology, biochemistry and pharmacology* 155–210 (Pergamon, 1985).
 68. Keeley, L. L. in *Comprehensive insect physiology, biochemistry and pharmacology* Vol. 3 211–248 (Pergamon, 1985).
 69. Wyatt, G. R. in *Insect biology in the future* 201–225 (Academic, 1980).
 70. Yi, Y. et al. Transgenerational accumulation of methylome changes discovered in commercially reared honey bee (*Apis mellifera*) queens. *Insect Biochem. Mol. Biol.* **127**, 103476 (2020).
 71. Parkhomchuk, D. et al. Transcriptome analysis by strand-specific sequencing of complementary DNA. *Nucleic Acids Res.* **37**, e123 (2009).
 72. Mortazavi, A., Williams, B. A., McCue, K., Schaeffer, L. & Wold, B. Mapping and quantifying mammalian transcriptomes by RNA-Seq. *Nat. Methods* **5**, 621–628 (2008).
 73. Anders, S. & Huber, W. Differential expression analysis for sequence count data. *Genome Biol.* **11**, R106 (2010).
 74. Robinson, M. D., McCarthy, D. J. & Smyth, G. K. edgeR: a Bioconductor package for differential expression analysis of digital gene expression data. *Bioinformatics* **26**, 139–140 (2010).
 75. Love, M. I., Huber, W. & Anders, S. Moderated estimation of fold change and dispersion for RNA-seq data with DESeq2. *Genome Biol.* **15**, 1–21 (2014).
 76. Kanehisa, M. & Goto, S. KEGG: kyoto encyclopedia of genes and genomes. *Nucleic Acids Res.* **28**, 27–30 (2000).
 77. Buenrostro, J. D., Giresi, P. G., Zaba, L. C., Chang, H. Y. & Greenleaf, W. J. Transposition of native chromatin for fast and sensitive epigenomic profiling of open chromatin, DNA-binding proteins and nucleosome position. *Nat. Methods* **10**, 1213–1218 (2013).
 78. Corces, M. R. et al. An improved ATAC-seq protocol reduces background and enables interrogation of frozen tissues. *Nat. Methods* **14**, 959–962 (2017).
 79. Bajic, M., Maher, K. A. & Deal, R. B. in *Plant chromatin dynamics: Methods and protocols* (eds Marian Bemer & Céilia Baroux) 183–201 (Springer New York, 2018).
 80. Yu, G., Wang, L.-G. & He, Q.-Y. ChIPseeker: an R/Bioconductor package for ChIP peak annotation, comparison and visualization. *Bioinformatics* **31**, 2382–2383 (2015).
 81. Schmehl, D. R., Tomé, H. V., Mortensen, A. N., Martins, G. F. & Ellis, J. D. Protocol for the in vitro rearing of honey bee (*Apis mellifera* L.) workers. *J. Apic. Res.* **55**, 113–129 (2016).

82. Kaftanoglu, O., Linksvayer, T. A. & Page, R. E. Jr Rearing honey bees, *Apis mellifera*, in vitro I: Effects of sugar concentrations on survival and development. *J. Insect Sci.* **11**, 96 (2011).
83. Han, B. et al. The molecular basis of socially induced egg-size plasticity in honey bees. *Elife* **11**, e80499 (2022).
84. Pan, L.-X., Hu, W.-W., Cheng, F.-P., Hu, X.-F. & Wang, Z.-L. Transcriptome analysis reveals differentially expressed genes between the ovary and testis of the honey bee *Apis mellifera*. *Apidologie* **53**, 15 (2022).
85. Vandesompele, J. et al. Accurate normalization of real-time quantitative RT-PCR data by geometric averaging of multiple internal control genes. *Genome Biol.* **3**, 1–12 (2002).
86. Hao, Y. et al. Integrated analysis of multimodal single-cell data. *Cell* **184**, 3573–3587. e3529 (2021).
87. Osborne, P. & Dearden, P. K. Non-radioactive in-situ hybridisation to honeybee embryos and ovaries. *Apidologie* **36**, 113–118 (2005).

Acknowledgements

This work was supported by the National Key R&D Program Project of China (2022YFD1600202), the National Natural Science Foundation of China (32172790) and the Earmarked Fund for China Agriculture Research System (CARS-44-KXJ15), and the Open Fund of Jiangxi Province Key Laboratory of Honeybee Biology and Beekeeping. Thanks to Prof. Zachary Y. Huang for his help in data analysis, drawing, and grammar.

Author contributions

Conceptualization: L.P., and Z.Z.; methodology: L.P., Z.W., and S.Z.; Investigation: L.P., Z.W., S.Z., T.X., W.C., and F.C.; formal analysis: L.P., T.X., W.C., and F.C.; writing—original draft, L.P.: Z.W., and Z.Z.; writing—review & editing: L.P., S.Z., and Z.Z.; visualization: L.P.; supervision: L.P., and Z.Z.; funding acquisition: Z.Z.; resources: Z.Z.; project administration: Z.Z.

Competing interests

The authors declare no competing interests.

Additional information

Supplementary information The online version contains supplementary material available at <https://doi.org/10.1038/s42003-025-08526-6>.

Correspondence and requests for materials should be addressed to Zhijiang Zeng.

Peer review information *Communications Biology* thanks Samir Moura Kadri, Duan C. Copeland and the other, anonymous, reviewer(s) for their contribution to the peer review of this work. Primary Handling Editors: John Mulley and Joao Valente.

Reprints and permissions information is available at <http://www.nature.com/reprints>

Publisher's note Springer Nature remains neutral with regard to jurisdictional claims in published maps and institutional affiliations.

Open Access This article is licensed under a Creative Commons Attribution-NonCommercial-NoDerivatives 4.0 International License, which permits any non-commercial use, sharing, distribution and reproduction in any medium or format, as long as you give appropriate credit to the original author(s) and the source, provide a link to the Creative Commons licence, and indicate if you modified the licensed material. You do not have permission under this licence to share adapted material derived from this article or parts of it. The images or other third party material in this article are included in the article's Creative Commons licence, unless indicated otherwise in a credit line to the material. If material is not included in the article's Creative Commons licence and your intended use is not permitted by statutory regulation or exceeds the permitted use, you will need to obtain permission directly from the copyright holder. To view a copy of this licence, visit <http://creativecommons.org/licenses/by-nc-nd/4.0/>.

© The Author(s) 2025